Contribution from the Department of Chemistry, North Carolina State University, Raleigh, North Carolina 27695-8204, and Chemistry and Materials Science Divisions, Argonne National Laboratory, Argonne, Illinois 60439

Simulation of Crystal Structures by Empirical Atom–Atom Potentials. 3. Effects of Oxygen Atom Vacancies on the Crystal Structure and the Superconducting Transition Temperature of the High-Temperature Superconductor $YBa_2Cu_3O_{7-y}$

Myung-Hwan Whangbo,*† Michel Evain,† Mark A. Beno,‡ Urs Geiser,‡ and Jack M. Williams*‡

Received September 4, 1987

The $YBa_2Cu_3O_{7-y}$ phase shows structural properties that are sensitively dependent upon the oxygen content of the Cu1 atom plane. These structural characteristics of $YBa_2Cu_3O_{7-y}$ were reproduced by employing the empirical atom–atom potentials derived from the binary oxides BaO, CuO, and Y_2O_3. The structural characteristics of $YBa_2Cu_3O_{7-y}$ stem essentially from the anisotropic oxygen atom environment around each Ba^{2+} cation (i.e., the Cu1 atom plane contains fewer O^{2-} anions than does the Cu2 atom plane), the extent of which increases with decreasing the oxygen content of the Cu1 atom plane. As the oxygen content of the Cu1 atom plane decreases, the O4 atom moves closer to and the Ba^{2+} cation moves farther away from the Cu1 atom plane, so that the $Ba^{2+}\cdots Ba^{2+}$ distance increases steadily thereby leading to an increase in the unit cell c parameter while the Cu1–O4 and Cu2–O4 distances sharply decrease and increase, respectively. The superconducting transition temperature (T_c) of $YBa_2Cu_3O_{7-y}$ is sharply lowered and eventually reaches zero as the oxygen content of the Cu1 atom plane is decreased. As a function of the oxygen content of the Cu1 atom plane, the T_c lowering follows the Cu1–O4 distance shortening and the Cu2–O4 distance lengthening so that the interaction between the CuO_2 layers which occurs in each $Ba_2Cu_3O_{7-y}^{3-}$ slab via the Cu2–O4–Cu1–O4–Cu2 linkages is essential for the high-T_c superconductivity in $YBa_2Cu_3O_{7-y}$. A consequence of weakening the interlayer interaction is to make the CuO_2 layers of each $Ba_2Cu_3O_{7-y}^{3-}$ slab independent and thus similar in electronic structure to the CuO_4 layers of the doped superconductors $La_{2-x}M_xCuO_4$ (M = Ba, Sr; $x \simeq 0.1$–0.2; $T_c \simeq 30$–40 K), thereby lowering the T_c of $YBa_2Cu_3O_{7-y}$ to ~55 K for $y \simeq 0.40$–0.50. Therefore, the superconductivity at $T_c \simeq 93$ K in $YBa_2Cu_3O_{7-y}$ for $y \simeq 0.15$–0.25 seems to involve Cooper pair formation between the electrons of the Cu2 atoms across the Cu2–O4–Cu1–O4–Cu2 linkages. The disappearance of superconductivity in tetragonal $YBa_2Cu_3O_{7-y}$ ($y > 0.5$) could be explained if its $x^2 - y^2$ bands remain half-filled, which can be achieved when the Cu1 atom plane contains Cu^{3+} and Cu^+ cations in the $(1-y):y$ ratio. The present simulation study suggests that formation of CuO_3 chains in $YBa_2Cu_3O_{7-y}$ ($y < 0.5$), which gives rise to an orthorhombic structure, may arise from two energy factors: to avoid a right-angle arrangement of oxygen atoms around Cu1 in the Cu1 atom plane and to avoid a T-shape three-coordinate geometry for copper. The same energy factors may still be at work in tetragonal $YBa_2Cu_3O_{7-y}$ ($y > 0.5$), in which the presence of enough oxygen atom vacancies may allow random formation of some short CuO_3 chains, and hence some Cu^{3+} sites, in two orthogonal directions, thereby leading to a tetragonal structure on a statistical basis.

The Y–Ba–Cu–O phase with a superconducting transition temperature (T_c) greater than 90 K[1] has been shown to be orthorhombic $YBa_2Cu_3O_{7-y}$ by a number of powder neutron diffraction studies.[2] This high-T_c superconductor consists of two-dimensional structural units, i.e., $Ba_2Cu_3O_{7-y}^{3-}$ slabs, that alternate with layers of Y^{3+} cations along the crystallographic c axis as illustrated in Figure 1.[3] Substitution of Y by lanthanide elements Ln (e.g., Ln = Sm, Eu, Gd, Dy, Ho, Yb) has little effects on the high-T_c superconductivity,[4] indicating that the $Ba_2Cu_3O_{7-y}^{3-}$ slabs are essential for the occurrence of the high-T_c superconductivity in $LBa_2Cu_3O_{7-y}$ (L = Y, Ln). In each $Ba_2Cu_3O_{7-y}^{3-}$ slab, two CuO_2 layers sandwich one CuO_3 chain and two Ba^{2+} cations per unit cell such that the copper atoms (Cu2) of the CuO_2 layers are capped by the oxygen atoms O4 of the CuO_3 chains to form the Cu2–O4–Cu1–O4–Cu2 linkages. Band electronic structure calculations show[3,5] that slight displacement of the capping oxygen atom, O4, from its equilibrium position causes slight valence fluctuations of the copper atoms, and gives rise to interactions between the two separated CuO_2 layers within each $Ba_2Cu_3O_{7-y}^{3-}$ slab. Hence lattice vibrational modes involving the capping oxygen atoms, O4, can bring about effective interactions between the CuO_2 layers.[5]

The partial oxygen atom vacancies of orthorhombic $YBa_2Cu_3O_{7-y}$ ($y < 0.5$) occur primarily at the O1 positions of the CuO_3 chains,[2a,b] i.e., the $(0, {}^1/_2, 0)$ sites of Figure 1. Orthorhombic $YBa_2Cu_3O_{7-y}$ undergoes a phase transition to a tetragonal structure as y increases beyond ~0.5 upon increasing temperature.[6] In tetragonal $YBa_2Cu_3O_{7-y}$ ($y > 0.5$), the empty sites $({}^1/_2, 0, 0)$ of Figure 1 are as equally occupied by oxygen atoms as are the O1 sites with a site population less than 0.25. Therefore, the tetragonal phase no longer has the CuO_3 chains found in the orthorhombic phase. The T_c of orthorhombic $YBa_2Cu_3O_{7-y}$ ($y < 0.5$) decreases with increasing y and drops precipitously at the orthorhombic to tetragonal (O → T) transition,[7a] and tetragonal $YBa_2Cu_3O_{7-y}$ does not appear to be superconducting.[7] Consequently, the presence of the CuO_3 chains is an important factor for the occurrence of the high-T_c superconductivity within each $Ba_2Cu_3O_{7-y}^{3-}$ slab.

The average coordination number of the Cu1 atom is very small (less than three) in tetragonal $YBa_2Cu_3O_{7-y}$, which lowers the

†North Carolina State University.
‡Argonne National Laboratory.

(1) Wu, M. K.; Ashburn, J. R.; Torng, C. J.; Hor, P. H.; Meng, R. L.; Gao, L.; Huang, Z. J.; Wang, Y. Q.; Chu, C. W. *Phys. Rev. Lett.* **1987**, *58*, 908.
(2) (a) Beno, M. A.; Soderholm, L.; Capone, D. W., II; Hinks, D. G.; Jorgensen, J. D.; Schuller, I. K.; Segre, C. U.; Zhang, K.; Grace, J. D. *Appl. Phys. Lett.* **1987**, *51*, 57. (b) Greedan, J. E.; O'Reilly, A.; Stager, C. V. *Phys. Rev. B: Condens. Matter* **1987**, *37*, 8770. (c) Capponi, J. J.; Chaillout, C.; Hewat, A. W.; Lejay, P.; Marezio, M.; Nguyen, N.; Raveau, B.; Soubeyroux, J. L.; Tholence, J. L.; Tournier, R. *Europhys. Lett.* **1987**, *3*, 1301. (d) David, W. I. F.; Harrison, W. T. A.; Gunn, J. M. F.; Moze, O.; Soper, A. K.; Day, P.; Jorgensen, J. D.; Beno, M. A.; Capone, D. W., II; Hinks, D. G.; Schuller, I. K.; Soderholm, L.; Segre, C. U.; Zhang, K.; Grace, J. D. *Nature* **1987**, *327*, 310. (e) Beech, F.; Miraglia, S.; Santoro, A.; Roth, R. S. *Phys. Rev. B: Condens. Matter* **1987**, *35*, 8778. (f) Hewat, A. W.; Capponi, J. J.; Chaillout, C.; Marezio, M.; Hewat, E. A. *Solid State Commun.* **1987**, *64*, 301.
(3) Whangbo, M.-H.; Evain, M.; Beno, M. A.; Williams, J. M. *Inorg. Chem.* **1987**, *26*, 1831.
(4) (a) Fisk, Z.; Thompson, J. D.; Zirngiebl, E.; Smith, J. L.; Cheong, S.-W. *Solid State Commun.* **1987**, *62*, 743. (b) Porter, L. C.; Thorn, R. L.; Geiser, U.; Umezawa, A.; Wang, H. H.; Kwok, W. K.; Kao, H.-C.; Monaghan, M. R.; Crabtree, G. W.; Carlson, K. D.; Williams, J. M. *Inorg. Chem.* **1987**, *26*, 1645. (c) Engler, E. M.; Lee, V. Y.; Nazzal, A. I.; Beyers, R. B.; Lim, G.; Grant, P. M.; Parkin, S. S. P.; Ramirez, M. L.; Vazquez, J. E.; Savoy, R. J. *J. Am. Chem. Soc.* **1987**, *109*, 2848.
(5) Whangbo, M.-H.; Evain, M.; Beno, M. A.; Williams, J. M. *Inorg. Chem.* **1987**, *26*, 1832.
(6) (a) Jorgensen, J. D.; Beno, M. A.; Hinks, D. G.; Soderholm, L.; Volin, K. J.; Hitterman, R. L.; Grace, J. D.; Schuller, I. K.; Segre, C. U.; Zhang, K.; Kleefisch, M. S. *Phys. Rev. B: Condens. Matter* **1987**, *36*, 3608. (b) Miraglia, S.; Beech, F.; Santoro, A.; Tran Qui, D.; Sunshine, S. A.; Murphy, D. W., submitted for publication in *Mater. Res. Bull.* (c) Renault, A.; McIntyre, G. J.; Collin, G.; Pouget, J.-P.; Comes, R. *J. Phys. (Les Ulis, Fr.)* **1987**, *48*, 1407. (d) Santoro, A.; Miraglia, S.; Beech, F.; Sunshine, S. A.; Murphy, D. W.; Schneemeyer, L. F.; Waszczak, J. V. *Mater. Res. Bull.* **1987**, *22*, 1007. (e) Onoda, M.; Shamoto, S.-I.; Sato, M.; Hosoya, S. *Jpn. J. Appl. Phys.* **1987**, *26*, L876.
(7) (a) Jorgensen, J. D.; Veal, B. W.; Kwok, W. K.; Crabtree, G. W.; Umezawa, A.; Nowicki, L. J.; Paulikas, A. P. *Phys. Rev. B: Condens. Matter* **1987**, *36*, 5731. (b) Bordet, P.; Chaillout, C.; Capponi, J. J.; Chenavas, J.; Marezio, M. *Nature (London)* **1987**, *327*, 687.

0020-1669/88/1327-0467$01.50/0

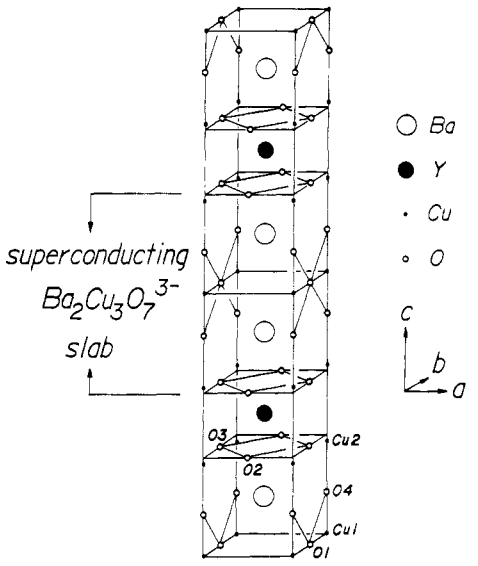

Figure 1. Crystal structure of orthorhombic $YBa_2Cu_3O_{7-y}$ ($y = 0.19$) as determined by powder neutron diffraction[2a]

d-block levels of the Cu1 atoms below those of the Cu2 atoms.[8] Hence the oxidation state of Cu1 is close to +1 in the tetragonal phase and close to +3 in the orthorhombic phase.[8] Nevertheless, the Cu1–O4 distance is shorter but the Cu2–O4 distance is longer in tetragonal than in orthorhombic $YBa_2Cu_3O_{7-y}$. According to our empirical atom–atom potential calculations,[9a] this result originates from the anisotropic oxygen atom environment around each Ba^{2+} cation. The O1 and ($^1/_2$, 0, 0) sites of Figure 1 belong to the Cu1 atom plane, while the O2 and O3 sites belong to the Cu2 atom plane. Thus the Cu1 atom plane contains fewer O^{2-} anions than does the Cu2 atom plane. The extent of this anisotropy increases with increasing oxygen atom vacancies of $YBa_2Cu_3O_{7-y}$ since it is primarily the oxygen atoms of the Cu1 atom plane that are lost.

In the present work we investigate the effect of the oxygen atom vacancies on the crystal structure of $YBa_2Cu_3O_{7-y}$ by performing empirical atom–atom potential calculations.[9,10] Our objective in the present study is to gain insight into the role of the oxygen atom vacancies in lowering T_c of $YBa_2Cu_3O_{7-y}$. In the following, we first describe the important structural characteristics of $YBa_2Cu_3O_{7-y}$ as determined by extensive powder neutron diffraction measurements.[2,6] Then we simulate these experimental observations in terms of the empirical atom–atom potentials[9] and discuss the implications of our results concerning the high-T_c superconductivity observed in $YBa_2Cu_3O_{7-y}$.

Structural Characteristics of $YBa_2Cu_3O_{7-y}$

Powder neutron diffraction measurements show[6a] that $YBa_2Cu_3O_{7-y}$ loses its oxygen content gradually with increasing temperature above 300 °C, which is shown in Figure 2. The O → T phase transition of $YBa_2Cu_3O_{7-y}$ is observed when $y \simeq 0.5$, which occurs near 700 °C in a pure oxygen atmosphere.[6a] In both orthorhombic and tetragonal $YBa_2Cu_3O_{7-y}$, it is the oxygen atoms of the Cu1 atom plane that are primarily lost upon raising the temperature.[6a] From numerous powder neutron diffraction studies,[2,6] crystal structures of $YBa_2Cu_3O_{7-y}$ at room temperature are known for various values of $y = 0.0$–1.0. On the basis of those structures, we identify and characterize the structural parameters of $YBa_2Cu_3O_{7-y}$ that depend sensitively upon the oxygen atom vacancies. The extent of oxygen atom vacancies can be measured by the overall oxygen content, $(7 - y)$, or by the oxygen content of the Cu1 atom plane, $(1 - y)$, which includes only the oxygen atom occupancies at the O1 and ($^1/_2$, 0, 0) sites. Since the oxygen atom vacancies of $YBa_2Cu_3O_{7-y}$ occur primarily at the O1 and ($^1/_2$, 0, 0) sites of the Cu1 atom plane, a change in the overall oxygen content is nearly the same as that in the oxygen content of the Cu1 atom plane. For instance, the $(7 - y)$ and $(1 - y)$ values of $YBa_2Cu_3O_{7-y}$ are respectively found to be 7.0 and 1.0,[2c,e] 6.81 and 0.92,[2a] 6.80 and 1.0,[2d] 6.80 and 0.80,[2e] 6.79 and 0.77,[2f] 6.7 and 0.7,[2b] 6.5 and 0.5,[6b] 6.26 and 0.26,[6c] 6.07 and 0.06,[6e] and 6.0 and 0.0.[6e] In the following we analyze the crystal structures of $YBa_2Cu_3O_{7-y}$ in terms of the $(1 - y)$ values, since these values are more meaningful as will be shown later.

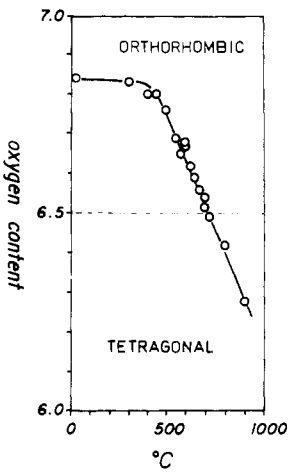

Figure 2. Overall oxygen content versus temperature for $YBa_2Cu_3O_{7-y}$ in a pure oxygen atmosphere (adapted from ref 6a).

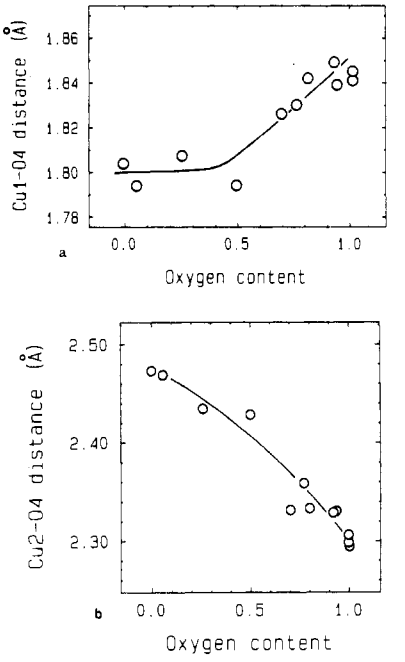

Figure 3. Cu1–O4 and Cu2–O4 distances of $YBa_2Cu_3O_{7-y}$ versus oxygen content of the Cu1 atom plane, $(1 - y)$, constructed from the data of ref 2 and 6: (a) Cu1–O4 distance vs oxygen content; (b) Cu2–O4 distance vs oxygen content.

Figure 3a shows the variation of the Cu1–O4 distance of $YBa_2Cu_3O_{7-y}$ as a function of the oxygen content of the Cu1 atom plane, $(1 - y)$. For y less than 0.5 the Cu1–O4 distance decreases sharply with increasing y, whereas it remains roughly constant for y greater than 0.5. Figure 3b shows that the Cu2–O4 distance of $YBa_2Cu_3O_{7-y}$ increases sharply with y for the entire region of

(8) Whangbo, M.-H.; Evain, M.; Beno, M. A.; Geiser, U.; Williams, J. M. *Inorg. Chem.* **1987**, *26*, 2566.
(9) (a) Evain, M.; Whangbo, M.-H.; Beno, M. A.; Williams, J. M. *J. Am. Chem. Soc.*, in press. (b) Evain, M.; Whangbo, M.-H.; Beno, M. A.; Geiser, U.; Williams, J. M. *J. Am. Chem. Soc.*, in press.
(10) (a) Stoneham, A. M.; Harding, J. H. *Annu. Rev. Phys. Chem.* **1986**, *37*, 53. (b) *Computer Simulation of Solids*; Catlow, C. R. A.; Mackrodt, W. C., Eds.; Springer-Verlag: New York, 1982. (c) Williams, D. E. *Top. Curr. Phys.* **1981**, *26*, 3. (d) Mirsky, K. In *Computing in Crystallography*; Delft University Press: Twente, The Netherlands, 1978; p 169.

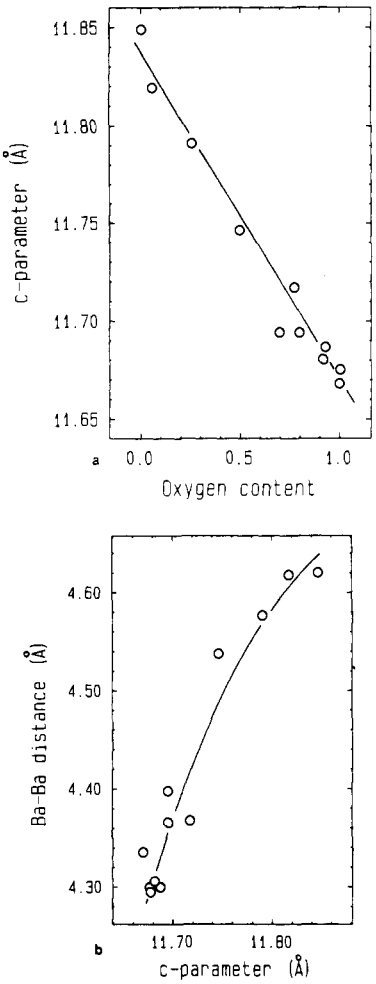

Figure 4. (a) c parameter of $YBa_2Cu_3O_{7-y}$ as a function of the oxygen content of the Cu1 atom plane, $(1 - y)$, and (b) Ba···Ba distance versus c parameter of $YBa_2Cu_3O_{7-y}$ (constructed from the data of ref 2 and 6).

y values. As a function of y, the change in the Cu2–O4 distance is greater than that in the Cu1–O4 distance by a factor of ~4. Thus the Cu2–O4–Cu1–O4–Cu2 linkage is lengthened as y increases. Consequently, with increasing y, the c parameter of $YBa_2Cu_3O_{7-y}$ increases gradually in the entire region of y as depicted in Figure 4a. The c parameter can be expressed as the sum of the Ba^{2+}···Ba^{2+} distance plus twice the Ba^{2+}···Y^{3+} distance. As a function of y, the Ba^{2+}···Y^{3+} distance does not change significantly. As shown in Figure 4b, the increase in the c parameter is due largely to that in the Ba^{2+}···Ba^{2+} distance. The structural characteristics summarized in Figures 3 and 4 can be traced back to the changes in the positional (crystallographic) z parameters of the O4 and Ba atoms: As shown in Figure 5, the z parameter of O4 gradually decreases while that of Ba gradually increases as the oxygen content decreases. That is, the O4 atom moves closer to the Cu1 atom plane but the Ba atom moves farther away from the Cu1 atom plane with decreasing oxygen content. Figure 5 also shows the average values of the O2 and O3 atom z parameters of orthorhombic $YBa_2Cu_3O_{7-y}$ and the O2 atom z parameters of tetragonal $YBa_2Cu_3O_{7-y}$. Figure 5 suggests that the oxygen atom plane of the CuO_2 layer gradually moves away from the Cu1 atom plane as the oxygen content decreases.

Simulation of the $YBa_2Cu_3O_{7-y}$ Structure

Empirical atom–atom potentials provide a practical tool for estimating the energies of crystalline solids.[10] By performing empirical atom–atom potential calculations, we recently examined the energetics of the O → T transition in La_2CuO_4[9b] and also the structural differences in orthorhombic $YBa_2Cu_3O_7$ and tetragonal $YBa_2Cu_3O_{6.5}$.[9a] In the present section, we employ this approach to simulate the crystal structures of $YBa_2Cu_3O_{7-y}$ as a function of y.

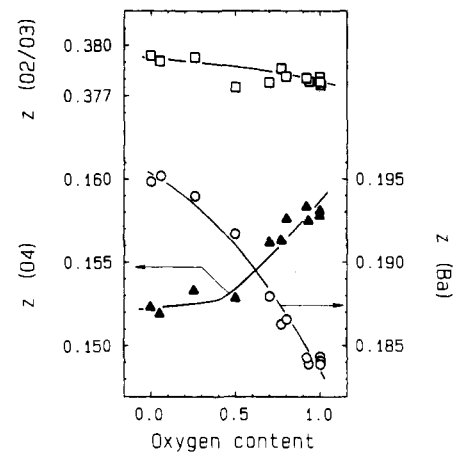

Figure 5. Positional z parameters of the O4, Ba, and O2/O3 atoms of $YBa_2Cu_3O_{7-y}$ as a function of the oxygen content of the Cu1 atom plane, $(1 - y)$, constructed from the data of ref 2 and 6.

Table I. Atom–Atom Potential Parameters of the O^{2-}···O^{2-}, Cu^{2+}···Cu^{2+}, La^{3+}···La^{3+}, Ba^{2+}···Ba^{2+}, and Y^{3+}···Y^{3+} Pairs

pair	B, eV	ρ, Å	C, eV Å^6
O^{2-}···O^{2-}	1387.7	0.375	63.31
Cu^{2+}···Cu^{2+}	269.10	0.264	0.5586
La^{3+}···La^{3+}	28855	0.250	325.0
Ba^{2+}···Ba^{2+}	3749.5	0.350	442.1
Y^{3+}···Y^{3+}	6902.5	0.250	18.44

Table II. Experimental and Calculated Values for the Unit Cell and Atom Positional Parameters of CuO, La_2O_3, BaO, and Y_2O_3[a,b]

CuO[c]	La_2O_3[d]	BaO[e]	Y_2O_3[f]
monoclinic	trigonal	cubic	cubic
($C2/c$)	($P\bar{3}m1$)	(NaCl)	($Ia3$)
a = 4.6516	a = 3.930	a = 5.523	a = 10.604
(−0.0321)	(−0.029)	(0.000)	(0.020)
b = 3.3582	c = 6.120		x(Y2) = −0.0314
(−0.0644)	(0.196)		(0.0017)
c = 5.1521	z(La) = 0.235		x(O) = 0.389
(0.0233)	(0.012)		(0.003)
β = 97.72	z(O) = 0.630		y(O) = 0.150
(−1.82)	(0.032)		(0.004)
z(O) = 0.4249			z(O) = 0.377
(0.0065)			(0.005)

[a] The experimental values are the numbers without parentheses. The numbers in the parentheses refer to the deviations of the calculated values from the corresponding experimental ones. [b] The cell parameters a, b, and c are in units of Å, and the angle β is in units of degrees. [c] reference 18. [d] Reference 19. [e] Reference 20. [f] Reference 21.

A. Method. For a pair of atoms i and j separated by the distance r_{ij} with the charges of q_i and q_j, respectively, their interaction energy W_{ij} may be written as[10]

$$W_{ij} = q_iq_j/r_{ij} + B_{ij}\exp(-r_{ij}/\rho_{ij}) - C_{ij}/r_{ij}^6 \qquad (1)$$

where the first, the second, and the third terms are the Coulomb, the nonbonded repulsion, and the van der Waals interaction energies, respectively. The constants B, ρ, and C are adjustable parameters to be determined on the basis of experimental data. These constants between different kinds of atoms may be related to those between identical atoms by[10]

$$B_{ij} = (B_{ii}B_{jj})^{1/2} \qquad 1/\rho_{ij} = (1/\rho_{ii} + 1/\rho_{jj})/2$$
$$C_{ij} = (C_{ii}C_{jj})^{1/2} \qquad (2)$$

With eq 1 and 2, we obtained from the program WMIN[11] the B, ρ, and C parameters for the O^{2-}···O^{2-}, Ba^{2+}···Ba^{2+}, Cu^{2+}···Cu^{2+}, La^{3+}···La^{3+}, and Y^{3+}···Y^{3+} pairs (listed in Table I) that reproduce

(11) Busing, W. R. "WMIN, A computer program to model molecules and crystals in terms of potential energy functions", Report ORNL-5497; Oak Ridge National Laboratory: Oak Ridge, TN, 1981.

Table III. Experimental and Calculated Values for the Unit Cell and Atom Positional Parameters of Orthorhombic La_2CuO_4, Tetragonal La_2CuO_4, Orthorhombic $YBa_2Cu_3O_{7-y}$, and Tetragonal $YBa_2Cu_3O_{7-y}$[a,b]

La_2CuO_4[c]	La_2CuO_4	$YBa_2Cu_3O_7$[d]	$YBa_2Cu_3O_{6.5}$[e]
orthorhombic	tetragonal	orthorhombic	tetragonal
(*Cmca*)	(*I4/mmm*)	(*Pmmm*)	(*P4/mmm*)
a = 5.3562 (−0.0078)	a = 3.7945	a = 3.8231 (0.1092)	a = 3.9018 (0.0729)
b = 13.1669 (0.1015)	c = 13.1205	b = 3.8863 (−0.0428)	c = 11.9403 (0.0371)
c = 5.3990 (0.0129)	z(La) = 0.3633	c = 11.6809 (0.1040)	z(Ba) = 0.1914 (0.0001)
y(La) = 0.3613 (0.0011)	z(O2) = 0.1827	z(Ba) = 0.1843 (0.0036)	z(Cu2) = 0.3590 (−0.0018)
z(La) = 0.0061 (0.0018)		z(Cu2) = 0.3556 (−0.0192)	z(O2) = 0.3792 (0.0005)
y(O1) = 0.0070 (0.0056)		z(O2) = 0.3773 (−0.0012)	z(O4) = 0.1508 (−0.0205)
y(O2) = 0.1842 (−0.0007)		z(O3) = 0.3789 (−0.0028)	
z(O2) = −0.0336 (−0.0153)		z(O4) = 0.1584 (0.0074)	

[a] Except for tetragonal La_2CuO_4, experimental values are the numbers without parentheses. The numbers in the parentheses refer to the deviations of the calculated values from the corresponding experimental ones. [b] The unit cell parameters are in units of Å. [c] Reference 14. [d] The experimental values are taken from orthorhombic $YBa_2Cu_3O_{6.81}$.[2a] [e] The experimental values are taken from tetragonal $YBa_2Cu_3O_{6.42}$.[6a]

the crystal structures of CuO, BaO, La_2O_3, and Y_2O_3.[9] In those WMIN calculations, the crystal energies are computed as a function of the unit cell and atom positional parameters in order to derive the optimum B, ρ, and C parameters. As shown in Table II,[12] the crystal structures of BaO, CuO, La_2O_3, and Y_2O_3 are well reproduced by use of the B, ρ and C parameters of Table I. The usefulness of these parameters depends upon how well they describe the crystal structures of other solids not included in the parameter determination.

B. Approximations and Utility of the Potential Parameters. Table III shows that the crystal structure of orthorhombic La_2CuO_4[13,14] is very well reproduced by the B, ρ, and C parameters of the $O^{2-}\cdots O^{2-}$, $Cu^{2+}\cdots Cu^{2+}$, and $La^{3+}\cdots La^{3+}$ pairs.[9b,12] Also listed in Table III are the optimum unit cell and atom positional parameters calculated for tetragonal La_2CuO_4,[9b] which are in close agreement with the corresponding experimental values of $La_{1.85}Ba_{0.15}CuO_4$[14] at room temperature. On the basis of the calculated crystal energies of the optimized orthorhombic and tetragonal La_2CuO_4 phase, the orthorhombic phase is predicted to be slightly more stable than the tetragonal phase (by 1.85 kcal/mol per unit cell),[9b] in agreement with experiment.[15]

$YBa_2Cu_3O_{7-y}$ consists of copper atoms with different oxidation states according to band electronic structure calculations.[3,5,8] It would be desirable to have different sets of B, ρ, and C values for copper···copper pairs of different oxidation states. However, this is impractical due to lack of appropriate copper oxides from which to refine different sets of B, ρ, and C parameters. Thus the B, ρ, and C values derived for the $Cu^{2+}\cdots Cu^{2+}$ pair may be used for all the copper···copper pairs of $YBa_2Cu_3O_{7-y}$ with the average oxidation state $2 + (1 - 2y)/3$ for all the copper atoms.[9a] These approximations are quite satisfactory in simulating the crystal structure of orthorhombic $YBa_2Cu_3O_7$ as shown in Table III.[9a,12]

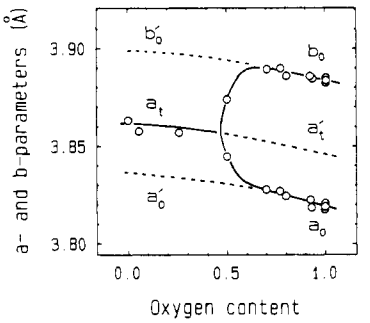

Figure 6. a and b parameters of $YBa_2Cu_3O_{7-y}$ versus oxygen content of the Cu1 atom plane, $1 - y$, where the subscripts o and t refer to the orthorhombic and tetragonal structures, respectively. The full lines refer to the data taken from ref 2 and 6, and the broken lines are hypothetical cell parameters extrapolated from the experimental ones.

The oxygen atom vacancies of $YBa_2Cu_3O_{7-y}$ occur primarily in the Cu1 atom plane,[2,6] so all the oxygen atom positions except for those of the Cu1 atom plane may be assumed to be fully occupied. The atom–atom pair interaction energies involving the partially occupied oxygen atom sites of the Cu1 atom plane may be evaluated as follows:[9a] For tetragonal $YBa_2Cu_3O_{7-y}$ all the O1 and ($^1/_2$, 0, 0) positions are regarded as fully occupied (i.e., 1.0 instead of $(1 - y)/2$), but the pair interaction energies involving each oxygen atom at either the O1 or the ($^1/_2$, 0, 0) sites are reduced in magnitude by a factor of $2/(1 - y)$ per such an oxygen atom. This treatment of the oxygen atom vacancies, which will be referred to as the average potential approximation in our later discussion, leads to results in good agreement with experiment as shown in Table III for tetragonal $YBa_2Cu_3O_{6.5}$.[9a,12] Thus the oxygen atom vacancies of orthorhombic $YBa_2Cu_3O_{7-y}$ can be treated in a similar manner. All the O1 sites are regarded as fully occupied (1.0 instead of 1− y), but the pair interaction energies involving each O1 atom are reduced in magnitude by a factor of $1/(1 - y)$ per such an oxygen atom.

C. Structural Effects of the Oxygen Atom Vacancies. The essential structural characteristics of $YBa_2Cu_3O_{7-y}$ described above originate from the z parameter behaviors of the O4, Ba and O2/O3 atoms as summarized in Figure 5, which we aim to reproduce by performing empirical atom–atom potential calculations. Thus, we calculate the optimum atom positional parameters of $YBa_2Cu_3O_{7-y}$ as a function of y by employing the program WMIN.[11] In this study, the unit cell parameters of $YBa_2Cu_3O_{7-y}$ are not optimized since our objective is to reproduce the qualitative trends in the atom positional parameters of Figure 5. Therefore we fixed the unit cell parameters of $YBa_2Cu_3O_{7-y}$ at certain values appropriate for y, as described below, and optimized only the atom positional parameters.

For various values of y, the c parameter of $YBa_2Cu_3O_{7-y}$ can be chosen from the straight line of Figure 4a. The full lines of Figure 6 indicate the manner in which the a and b parameters of orthorhombic $YBa_2Cu_3O_{7-y}$ (a_o and b_o, respectively) and the a parameter of tetragonal $YBa_2Cu_3O_{7-y}$ (a_t) vary as a function

(12) The calculated structures for CuO, orthorhombic La_2CuO_4, and orthorhombic $YBa_2Cu_3O_7$ do not represent minima but represent saddle points on the potential energy surfaces of five, eight, and eight structural parameter spaces, respectively, because the corresponding Hessian matrices give rise to two, one, and one negative eigenvalues, respectively. The present atom–atom potentials do not properly represent the energy changes associated with bond angle variations, since they completely neglect the potential covalent bonding between pairs of atoms and hence the effect of directed valence. With the present set of empirical atom–atom potentials, the minimum energy structures calculated for CuO, orthorhombic La_2CuO_4, and orthorhombic $YBa_2Cu_3O_7$ are very different from those observed and thus are physically meaningless. The structures of CuO, orthorhombic La_2CuO_4, and orthorhombic $YBa_2Cu_3O_7$ listed in Tables II and III are those we optimized by using only the linear combinations of the eigenfunctions of the Hessian matrices with the positive eigenvalues. As shown, the resulting structures are in excellent agreement with experiment, so the above contraint introduced in the WMIN program seems to serve as substitutes for the unknown extra potential energy terms yet to be determined. Since the Coulomb and nonbonded repulsion terms are probably the major forces involved, our conclusions concerning why and how the oxygen content of the Cu1 atom plane affects the z parameters of the O4, Ba, O2, and O3 atoms will remain valid.

(13) Grande, B.; Müller-Bauschbaum, H.; Schweizer, M. *Z. Anorg. Allg. Chem.* **1977**, *428*, 120.
(14) Jorgensen, J. D.; Schüttler, H.-B.; Hinks, D. G.; Capone, D. W., II; Zhang, K.; Brodsky, M. B.; Scalapino, D. J. *Phys. Rev. Lett.* **1987**, *58*, 1024.
(15) Longo, J. M.; Raccah, P. M. *J. Solid State Chem.* **1973**, *6*, 526.

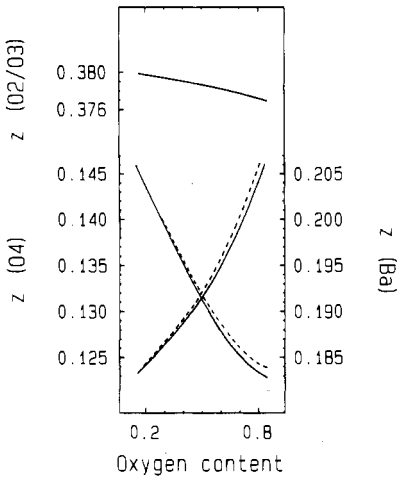

Figure 7. Calculated z parameters of O4, Ba, and O2/O3 atoms of $YBa_2Cu_3O_{7-y}$ versus oxygen content of the Cu1 atom, $(1 - y)$.

of the oxygen content of the Cu1 atom plane, $(1 - y)$. The dashed line a_t' may be considered as the a parameter of hypothetical tetragonal $YBa_2Cu_3O_{7-y}$ for y less than 0.5. Likewise, the dashed lines a_o' and b_o' may be considered as the a and b parameters of hypothetical orthorhombic $YBa_2Cu_3O_{7-y}$ for y greater than 0.5. With these approximations, we can assign the unit cell parameters of both orthorhombic and tetragonal $YBa_2Cu_3O_{7-y}$ for the entire region of $y = 0.0$–1.0.

Shown in Figure 7 are the z parameters of the O4, Ba, and O2/O3 atoms calculated for $YBa_2Cu_3O_{7-y}$ as a function of the oxygen content of the Cu1 atom plane, where the full and broken lines refer to the results obtained from orthorhombic and tetragonal $YBa_2Cu_3O_{7-y}$, respectively. For the z parameters of the O2/O3 atoms, the full and the broken lines practically overlap, and hence only the full line is shown. As the oxygen content decreases, Figure 7 shows that the z parameter of O4 gradually decreases, that of Ba gradually increases, and that of O2/O3 gradually increases slightly. These z parameter trends are identical with those observed experimentally (See Figure 5). It is significant that both orthorhombic and tetragonal $YBa_2Cu_3O_{7-y}$ lead to nearly identical results. Thus the z parameters behaviors of Figure 7 (and hence those of Figure 5) are mainly governed by the extent of the oxygen atom vacancies in the Cu1 atom plane, regardless of how these vacancies are distributed to give an orthorhombic or a tetragonal structure. In the remainder of this section, we discuss in some detail the z parameter trends of Figure 7 from the viewpoint of the oxygen atom vacancies.

For all values of $y \simeq 0.0$–1.0 in $YBa_2Cu_3O_{7-y}$, the oxygen atom environment of each Ba^{2+} cation is anisotropic in that the Cu1 atom plane contains fewer O^{2-} anions than does the Cu2 atom plane. Therefore, the Coulomb attraction of the Ba^{2+} cation and the Coulomb repulsion of the O4 atom with the O^{2-} anions of the Cu1 atom plane are smaller in magnitude than with those of the Cu2 atom plane.[9a] This explains why the Cu1–O4 distance is shorter than the Cu2–O4 distance and is in part responsible for the Ba^{2+}···Ba^{2+} distance being greater than the Ba^{2+}···Y^{3+} distance.

In $YBa_2Cu_3O_{7-y}$ the extent of the anisotropy of the oxygen atom environment around each Ba^{2+} cation increases as the overall oxygen content decreases because it is primarily the oxygen atoms of the Cu1 atom plane that are lost. Therefore, the Coulomb attraction of the Ba^{2+} cation and the Coulomb repulsion of the O4 atom toward the O^{2-} anions of the Cu1 atom plane become weaker with decreasing oxygen content. Consequently, the capping oxygen atom, O4, moves closer to while the Ba atoms and hence the CuO_2 layers move farther away from the Cu1 atom plane.[9a]

As the Ba^{2+} cation moves away from the Cu1 atom plane, the O2/O3 plane moves slightly away from the Cu1 atom plane (see the z parameters of the O2/O3 atoms in Figure 7), and the Ba^{2+}···Y^{3+} distance remains nearly constant for all values of $y = 0.0$–1.0 so that the gradual increase in the c parameter of $YBa_2Cu_3O_{7-y}$ with decreasing oxygen content is well correlated

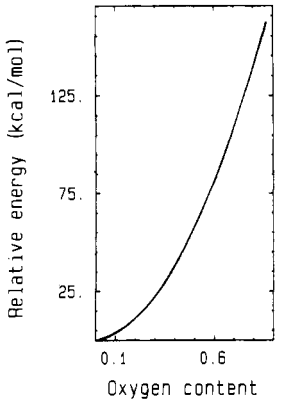

Figure 8. Calculated relative stability (kcal/mol per formula unit) of orthorhombic $YBa_2Cu_3O_{7-y}$ with respect to tetragonal $YBa_2Cu_3O_{7-y}$ as a function of the oxygen content of the Cu1 atom plane, $(1 - y)$.

with the corresponding increase in Ba^{2+}···Ba^{2+} distance, as shown in Figure 4b. The Cu1–O4 distance becomes shorter when the O4 atoms moves closer to the Cu1 atom plane with decreasing oxygen content. Below a certain minimum value (~1.80 Å), the Cu1–O4 distance cannot be further shortened due to a strong nonbonded repulsion between the oxygen and copper atoms involved. This accounts for the behavior of the Cu1–O4 distance as a function of the oxygen content shown in Figure 3a. As the Ba atoms move away from the Cu1 atom plane, so do the CuO_2 layers. Consequently, the Cu–O4 distance of $YBa_2Cu_3O_{7-y}$ increases steeply with increasing y.

D. Oxygen Atom Ordering in the Cu1 Atom Plane. The relative stability of orthorhombic $YBa_2Cu_3O_{7-y}$ with respect to tetragonal $YBa_2Cu_3O_{7-y}$ calculated as a function of the oxygen content by use of the empirical atom–atom potentials is plotted in Figure 8. The orthorhombic structure is calculated to be more stable than the tetragonal one for all values of y ($\neq 1$), and the relative stability decreases gradually with decreasing oxygen content. The huge stability difference between the two structures calculated for $y < 1$ results largely from the average potential approximation employed for the partially occupied oxygen atom sites of the Cu1 atom plane and points to an important implication concerning the nature of the oxygen atom ordering in that plane.

Provided that the maximum coordination number of each Cu1 atom in $YBa_2Cu_3O_{7-y}$ is four as in ideal orthorhombic $YBa_2Cu_3O_7$, each Cu1 atom of $YBa_2Cu_3O_{7-y}$ may have zero, one, or two oxygen atoms coordinated from the Cu1 atom plane as shown in **1**–**3**,

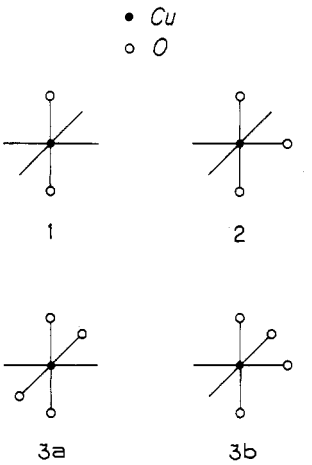

respectively. In **3a** and **3b** the oxygen atoms of the Cu1 atom plane have a linear and a right-angle arrangement around Cu1, respectively. Within the Cu1 atom plane, the oxygen atoms of **3b** have a shorter distance and hence a greater Coulomb repulsion between them than do the oxygen atoms of **3a**. In the average potential approximation, each Cu1 atom of tetragonal $YBa_2Cu_3O_{7-y}$ is surrounded by four oxygen atoms of the Cu1 atom plane thereby leading to four pairs of oxygen atoms with the

right-angle arrangement, whereas each Cu1 atom of orthorhombic $YBa_2Cu_3O_{7-y}$ has no such oxygen atom arrangement in the Cu1 atom plane. Therefore, it is understandable that the tetragonal phase is calculated to be significantly less stable than the orthorhombic phase.

As discussed above, the right-angle arrangement of oxygen atoms in the Cu1 atom plane (e.g., **3b**) is very unfavorable energetically. Therefore it is quite probable that the tetragonal phase of $YBa_2Cu_3O_{7-y}$ derived from powder neutron diffraction measurements reflects an average structure of random oxygen atom distributions in the Cu1 atom plane in which no Cu1 atom has the right-angle arrangement of oxygen atoms. Then a tetragonal structure of $YBa_2Cu_3O_{7-y}$ might be one in which the oxygen atoms of the Cu1 atom plane are randomly distributed under the two restrictions: (a) Oxygen atoms at the ($^1/_2$, 0, 0) sites are equal in number to those at the (0, $^1/_2$, 0) sites, and (b) no Cu1 atom has the right-angle arrangement of oxygen atoms around it from the Cu1 atom plane. The maximum oxygen content, N_{max}, allowed for the tetragonal structure of $YBa_2Cu_3O_{7-y}$ as defined above can be calculated by simulating the random oxygen atom distributions in the Cu1 atom plane by use of random number generation. Such a simulation shows N_{max} to be 6.73, at which value of $YBa_2Cu_3O_{7-y}$ the Cu1 atom plane is calculated to contain two-coordinate (linear, **1**), three-coordinate (T-shape, **2**), and four-coordinate (tetragonal, **3a**) copper atoms in a 1:53:46 ratio. Certainly, the statistical limit N_{max} = 6.73 is greater than 6.5, below which $YBa_2Cu_3O_{7-y}$ is experimentally observed to be tetragonal. Thus a certain energy factor should operate in $YBa_2Cu_3O_{7-y}$, which favors the orthorhombic structure in the region of $y < 0.5$.

The T-shape three-coordination has not been observed for copper and thus might be energetically unfavorable. The number of the T-shape three-coordinate copper atoms can be decreased by increasing the number of tetragonal four-coordinate copper atoms, which amounts to increasing the average length of the CuO_3 chains. Then it may be conjectured that the CuO_3 chain formation in $YBa_2Cu_3O_{7-y}$ for $y < 0.5$ originates from two energy factors: one to avoid the right-angle arrangement of oxygen atoms around each Cu1 atom within the Cu1 atom plane and the other to avoid the T-shape three-coordination of copper. Even for $y > 0.5$ where the tetragonal phase is found, the above two energy factors may still be at work. Thus one cannot exclude the possibility that, in tetragonal $YBa_2Cu_3O_{7-y}$, the presence of enough oxygen atom vacancies in the Cu1 atom plane allows short CuO_3 chains to form randomly in the two orthogonal directions of that plane thereby leading to a tetragonal structure on a statistical basis.

As discussed above, the Cu1 atom plane of $YBa_2Cu_3O_{7-y}$ would contain two-, three-, and four-coordination sites (**1**, **2**, and **3a**, respectively), the proportions of which depend upon the oxygen atom vacancies. The three sites would have different geometrical effects. For instance, the Cu1–O4 distances of **1**–**3** would increase in the order **1** < **2** < **3a** according to the Coulomb repulsions associated with the capping oxygen atoms O4 (see the previous section). Consequently, it is important to realize that the structural characteristics of $YBa_2Cu_3O_{7-y}$ summarized in Figures 3–5 refer to average quantities arising from different copper atom sites. For example, a shortening of the Cu1–O4 distance with decreasing oxygen content (see Figure 3a) does not mean that all the Cu1–O4 distances are equally shortened. Instead, it means that the portion of the copper atom sites with the long Cu1–O4 distance (e.g., **3a**) is decreased and that with the short Cu1–O4 distance (e.g., **1** or **2**) is increased, and thus the Cu1–O4 distance is shortened in terms of a statistical average. The Cu1–O4 and Cu2–O4 distances we discuss in the following sections refer to such statistically averaged quantities.

Oxygen Atom Content and T_c

When a sample of $YBa_2Cu_3O_{7-y}$ at a temperature T_Q is quenched (cooled rapidly), the resulting sample has a T_c value that depends upon T_Q.[7a,16] Thus T_c is about 93 K for T_Q < 500 °C, T_c decreases with increasing T_Q for 500 °C < T_Q < 790 °C, and T_c is zero for T_Q > 790 °C. The oxygen content of $YBa_2Cu_3O_{7-y}$ depends upon temperature as shown in Figure 2. To a first approximation, the quenched sample may be assumed to retain the oxygen content it had before quenching. Then by using Figure 2, one can deduce how the T_c value of $YBa_2Cu_3O_{7-y}$ varies as a function of its oxygen content from the available T_c vs T_Q data. This is shown in Figure 9, where the empty circles and empty triangles refer to the T_c vs T_Q data of van den Berg et al.[16] and Jorgensen et al.,[7a] respectively. The filled square and filled hexagon represent the results obtained by Katano et al.[17] and Beno et al.[2a] from slowly cooled samples. Plots of T_c vs the oxygen content similar to Figure 9 have been reported for quenched samples.[22-24] Figure 9 reveals that T_c of $YBa_2Cu_3O_{7-y}$ is nearly constant at about 93 K for $y \simeq 0.15$–0.25, decreases sharply with increasing y beyond 0.25 (see the full line), and is zero for $y > 0.5$. An apparent exception to this observation is the result of Katano et al.,[17] which shows $T_c \simeq 94$ K at $y = 0.40$. In the $YBa_2Cu_3O_{7-y}$ samples of Beno et al.[2a] and Jorgensen et al.,[6] the oxygen atom vacancies occur primarily in the Cu1 atom plane so that a change in the overall oxygen content, 7 − y, is nearly equal to that in the oxygen content, 1 − y, in the Cu1 atom plane. This is not the case, with the $YBa_2Cu_3O_{6.6}$ sample of Katano et al.,[17] since it has substantial oxygen atom vacancies in the Cu2 atom planes. The oxygen content in the Cu1 atom plane of this $YBa_2Cu_3O_{6.6}$ sample is 0.78. Therefore, what really controls the magnitude of T_c in $YBa_2Cu_3O_{7-y}$ is not the overall oxygen content but the oxygen content of the Cu1 atom plane. The data points of Figure 9 deviate from the full line most noticeably near $T_c \simeq$ 50–60 K. Recent studies on quenched $YBa_2Cu_3O_{7-y}$ samples show[22,23] that the T_c vs the oxygen content plot has two plateaus

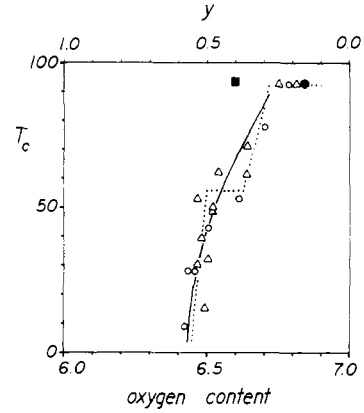

Figure 9. T_c versus overall oxygen content in $YBa_2Cu_3O_{7-y}$, where the empty circles and empty triangles represent the data of van den Berg et al.[16] and Jorgensen et al.,[7a] respectively. The filled square and filled hexagon refer to the data of Katano et al.[17] and Beno et al.,[2a] respectively.

(16) Van den Berg, J.; van der Beek, C. J.; Kes, P. H.; Nieuwenhuys, G. J.; Mydosh, J. A.; Zandbergen, H. W.; van Berkel, F. P. F.; Steens, R.; Ijdo, D. J. W. *Europhys. Lett.* **1987**, *4*, 737.
(17) Katano, S.; Funahashi, S.; Hatano, T.; Matsushita, A.; Nakamura, K.; Matsumoto, T.; Ogawa, K. *Jpn. J. Appl. Phys., Part 2* **1987**, *26*, L1046.
(18) Asbrink, S.; Norrby, L.-J. *Acta Crystallogr., Sect. B: Struct. Crystallogr. Cryst. Chem.* **1970**, *B26*, 8.
(19) (a) Pauling, L. *Z. Kirstallogr., Kristallgesn., Kristallphys., Kristallchem.* **1929**, *69*, 415. (b) Wyckoff, R. W. G. *Crystal Structures*, 2nd ed.; Wiley: New York, 1964; Vol. 2, Chapter V, Section A.
(20) Zollweg, R. J. *Phys. Rev.* **1955**, *100*, 671.
(21) O'Conner, B. H.; Valentine, T. M. *Acta Crystallogr. Sect. B: Struct. Crystallogr. Cryst. Chem.* **1969**, *B25*, 2140.
(22) (a) Veal, B. W.; Jorgensen, J. D.; Crabtree, G. W.; Kwok, W.; Umezawa, A.; Paulikas, A. P.; Morss, L. R.; Appelman, E. H.; Nowicki, L. J.; Nuñez, L.; Claus, H. Presented at the International Conference on Electronic Structure and Phase Stability in Advanced Ceramics; Argonne National Laboratory, Argonne, IL, 1987. (b) Johnston, D. C.; Jacobson, A. J.; Newsam, J. M.; Lewandowski, J. T.; Goshorn, D. P.; Xie, D.; Yelon, W. B. Presented at the Symposium on Inorganic Superconductors, 194th National Meeting of the American Chemical Society, New Orleans, LA, August 31–September 4, 1987.
(23) Cava, R. J.; Batlogg, B.; Chen, C. H.; Rietman, E. A.; Zahurak, S. M.; Werder, D. *Phys. Rev. B: Condens. Matter* **1987**, *36*, 5719.
(24) Appelman, E. H.; Morss, L. R.; Kini, A. M.; Geiser, U.; Umezawa, A.; Crabtree, G. W.; Carlson, K. D. *Inorg. Chem.* **1987**, *26*, 3237.

as depicted by the dotted lines in Figure 9 (e.g., one plateau at $T_c \simeq 93$ K for $y \simeq 0.15$–0.25, and the other at $T_c \simeq 55$ K for $y \simeq 0.40$–0.50).

We now examine how the plot of T_c vs the oxygen content shown in Figure 9 might be related to the structural and/or electronic properties of $YBa_2Cu_3O_{7-y}$ that depend upon the oxygen content of the Cu1 atom plane. In each $Ba_2Cu_3O_{7-y}^{3-}$ slab, the interaction between the CuO_2 layers occurs via the Cu2–O4–Cu1–O4–Cu2 linkages.[5,8] This interaction should be weakened as the Cu1–O4 distance shrinks and the Cu2–O4 distance elongates upon decreasing the oxygen content of the Cu1 atom plane (see Figure 3). Note that the plot of T_c vs the oxygen content shown in Figure 9 is quite similar in trend to that of the Cu1–O4 distance vs the oxygen atom content shown in Figure 3a. Therefore, it seems that the interaction between the CuO_2 layers in each $Ba_2Cu_3O_{7-y}^{3-}$ slab, which occurs via the Cu2–O4–Cu1–O4–Cu2 linkages, is essential for the high-T_c superconductivity and that the lowering of T_c in $YBa_2Cu_3O_{7-y}$ with decreasing oxygen content of the Cu1 atom plane is caused by the weakening of this interlayer interaction, which is brought about by the Cu1–O4 distance shortening and the Cu2–O4 distance elongation. We notice that, in the $YBa_2Cu_3O_{7-y}$ sample with $T_c \simeq 94$ K prepared by Katano et al.,[17] the Cu1–O4 distance is longer (i.e., 1.847 Å at 120 K) than one might expect from Figure 3a on the basis of its overall oxygen content of 6.6 alone. Again, this result is consistent with our conclusion that the high-T_c superconductivity of $YBa_2Cu_3O_{7-y}$ is intimately associated with the magnitude of the interaction between the CuO_2 layers, which occurs via the Cu2–O4–Cu1–O4–Cu2 linkages in each $Ba_2Cu_3O_{7-y}^{3-}$ slab.[5,8]

Decoupling of the Interlayer Interaction and Mixed Valence

Suppose that the Cu2–O4 distance of each $Ba_2Cu_3O_{7-y}^{3-}$ slab is increased beyond (also the Cu1–O4 distance is decreased below) a certain value, which occurs when enough four-coordination copper sites **3a** are removed from the Cu1 atom plane. Then the interaction between the CuO_2 layers occurring via the Cu2–O4–Cu1–O4–Cu2 linkages may become so weak that the CuO_2 layers would be independent of each other as are the CuO_4 layers in the doped superconductors $La_{2-x}M_xCuO_4$ (M = Ba, Sr),[25] which exhibit superconductivity at $T_c \simeq 30$–40 K for $x \simeq 0.1$–0.2. The T_c value of $La_{2-x}M_xCuO_4$ reaches ~53 K under an applied pressure of ~12 kbar,[26] and the partially filled $x^2 - y^2$ band of the CuO_4 layers in $La_{2-x}M_xCuO_4$[27] is essentially identical with that of the CuO_2 layers in $YBa_2Cu_3O_{7-y}$.[3,5,28] Consequently, for a certain range of y values (e.g., $y \simeq 0.4$–0.5), the CuO_2 layers of $YBa_2Cu_3O_{7-y}$ could become similar in electronic structure to the CuO_4 layers of $La_{2-x}M_xCuO_4$ under an applied pressure of ~12 kbar, which would be responsible for the lower plateau at $T_c \simeq 55$ K in the T_c vs oxygen plot of Figure 9 (see the dotted lines). This rationalization implies that the CuO_2 layer $x^2 - y^2$ band of $YBa_2Cu_3O_{7-y}$ for $y \simeq 0.4$–0.5 would have a band occupancy of 0.43, as does the CuO_4 layer $x^2 - y^2$ band of $La_{2-x}M_xCuO_4$ (M = Ba, Sr; $x \simeq 0.15$).

$La_{2-x}M_xCuO_4$ is not superconducting when its $x^2 - y^2$ band occupancy is close to 0.5 because of the electronic instability (i.e., an antiferromagnetic ordering) associated with the half-filled band.[27-29] By analogy, one might suggest that the absence of superconductivity in $YBa_2Cu_3O_{7-y}$ ($y > 0.5$) arises from its half-filled $x^2 - y^2$ band of the CuO_2 layers. For this to be true, a certain condition must be imposed on the copper atom valence states in the Cu1 atom plane. The copper atom oxidation state at the linear-coordination site **1** or at the three-coordination site **2** is likely to be +1,[8] while that at the four-coordination site **3a** is likely to be +3.[3,5,30] Thus the Cu1 atom plane would consist of Cu^{3+} and Cu^+ cations. If β is the fraction of the Cu^{3+} sites in the Cu1 atom plane, the average oxidation state, α_1, of the Cu1 atom is given by

$$\alpha_1 = 3\beta + (1 - \beta) = 2\beta + 1 \quad (3a)$$

The charge neutrality for $YBa_2Cu_3O_{7-y}$ requires that

$$\alpha_1 = 7 - 2y - 2\alpha_2 \quad (3b)$$

where α_2 is the average oxidation state of the Cu2 atom. From eq 3a and 3b

$$\beta = 3 - y - \alpha_2 \quad (4a)$$

$$\beta = 1 - y, \text{ if } \alpha_2 = 2 \quad (4b)$$

For the CuO_2 layers $x^2 - y^2$ band to be half-filled, eq 4b suggests that the fraction of the Cu^{3+} sites, β, in the Cu1 atom plane should decrease with increasing oxygen atom vacancies in that plane, eventually reaching zero at $y = 1.0$. Intuitively, this proposal seems quite reasonable.

Concluding Remarks

The structural characteristics of $YBa_2Cu_3O_{7-y}$ that depend upon the oxygen atom vacancies of the Cu1 atom plane are well reproduced by the empirical atom–atom potentials derived from the binary oxides BaO, CuO, and Y_2O_3.[9] Those structural characteristics originate essentially from the anisotropic oxygen atom environment around each Ba^{2+} cation; i.e., the Cu1 atom plane contains fewer O^{2-} anions than does the Cu2 atom plane. The extent of this anisotropy in $YBa_2Cu_3O_{7-y}$ increases with y since the oxygen atoms of the Cu1 atom plane are primarily removed upon increasing the temperature. Thus the Coulomb repulsion of the capping oxygen atom O4 with O^{2-} anions of the Cu1 atom plane decreases in magnitude as the number of oxygen atom vacancies of the Cu1 atom plane increases. Therefore, with decreasing oxygen content of the Cu1 atom plane, the Cu1–O4 and the Cu2–O4 distances of $YBa_2Cu_3O_{7-y}$ sharply decrease and increase, respectively. Since the change in the Cu2–O4 distance is much greater, the Cu2–O4–Cu1–O4–Cu2 linkage is lengthened as the oxygen content of the Cu1 atom plane decreases.

The two separated CuO_2 layers of each $Ba_2Cu_3O_{7-y}^{3-}$ slab interact via the Cu2–O4–Cu1–O4–Cu2 linkages.[3,5,8] Thus, the lowering of T_c in $YBa_2Cu_3O_{7-y}$ with decreasing the oxygen content of the Cu1 atom plane would be a result of weakening this interlayer interaction within each $Ba_2Cu_3O_{7-y}^{3-}$ slab, which is caused by the shortening of the Cu1–O4 distance and the lengthening of the Cu2–O4 distance. The extent of the interlayer interaction is weakened on a statistical basis, as the number of the four-coordinate copper sites **3a** is reduced by removing the O1 atoms from the Cu1 atom plane. An important consequence of weakening the interlayer interaction is to make the CuO_2 layers of each $Ba_2Cu_3O_{7-y}^{3-}$ slab independent, so that they become similar in electronic structure to the CuO_4 layers $La_{2-x}M_xCuO_4$. This could give rise to the lower plateau at ~55 K in the T_c vs oxygen content plot for $YBa_2Cu_3O_{7-y}$. The upper plateau of this plot at $T_c \simeq 93$ K suggests that the high-T_c superconductivity at $T_c \simeq 93$ K

(25) (a) Bednorz, J. G.; Muller, K. A. *Z. Phys. B.: Condens. Matter* **1986**, *64*, 189. (b) Uchida, S.; Takagi, H.; Kitazawa, K.; Tanaka, S. *Jpn. J. Appl. Phys., Part 2* **1987**, *26*, L1. (c) Takagi, H.; Uchida, S.; Kitazawa, K.; Tanaka, S. *Jpn. J. Appl. Phys., Part 2* **1987**, *26*, L123, L218. (d) Cava, R. J.; van Dover, R. B.; Batlogg, B.; Rietman, E. A. *Phys. Rev. Lett.* **1987**, *58*, 408. (e) Capone, D. W., II; Hincks, D. G.; Jorgensen, J. D.; Zhang, K. *Appl. Phys. Lett.* **1987**, *50*, 543.
(26) (a) Chu, C. W.; Hor, P. H.; Meng, R. L.; Gao, L.; Huang, Z. J.; Wang, Y. Q. *Phys. Rev. Lett.* **1987**, *58*, 405. (b) Chu, C. W.; Hor, P. H.; Meng, R. L.; Gao, L.; Huang, Z. J. *Science (Washington, D.C.)* **1987**, *235*, 567.
(27) Whangbo, M.-H.; Evain, M.; Beno, M. A.; Williams, J. M. *Inorg. Chem.* **1987**, *26*, 1829.
(28) Williams, J. M.; Beno, M. A.; Carlson, K. D.; Geiser, U.; Kao, H. C. I.; Kini, A. M.; Porter, L. C.; Schultz, A. J.; Thorn, R. J.; Wang, H. H.; Whangbo, M.-H.; Evain, M. *Acc. Chem. Res.*, in press.
(29) (a) Johnston, D. C.; Stokes, J. P.; Goshorn, D. P.; Lewandowski, J. T. *Phys. Rev. B: Condens. Matter* **1987**, *36*, 4007. (b) Mitsuda, S.; Shirane, G.; Sinha, S. K.; Johnston, D. C. *Phys. Rev. B: Condens. Matter* **1987**, *36*, 822. (c) Freltoft, T.; Remeika, J. P.; Moncton, D. E.; Cooper, A. S.; Fisher, J. E.; Harshman, D.; Shirane, G.; Sinha, S. K.; Vaknin, D. *Phys. Rev. B: Condens. Matter* **1987**, *36*, 826. (d) Kang, W.; Collin, G.; Ribault, M.; Friedel, J.; Jérome, D.; Bassat, J. M.; Coutures, J. P.; Odier, P. *J. Phys. (Les Ulis, Fr.)* **1987**, *48*, 1181.
(30) Whangbo, M.-H.; Evain, M.; Beno, M. A.; Williams, J. M. *Superconductivity: Synthesis, Properties, and Processing*; Hatfield, W. E., Ed.; Marcel Dekker: New York, in press.

is achieved when the proportion of the four-coordinate copper sites **3a** in the Cu1 atom plane exceeds a certain minimum value. An important implication of these observations is that the superconductivity at $T_c \simeq 93$ K might originate from the formation of Cooper pairs (i.e., pairs of electrons that are charge carriers of superconductors) between electrons of the Cu2 atoms across the Cu2-O4-Cu1-O4-Cu2 linkages as illustrated in **4**.[30] When

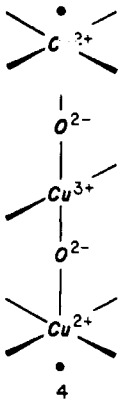

4

such a Cooper pair formation is unfavorable by lengthening the Cu2-O4-Cu1-O4-Cu2 linkages, Cooper pairs may be formed between the electrons of the Cu2 atoms within each CuO_2 layer, a situation identical with that in the CuO_4 layers of doped superconductors $La_{2-x}M_xCuO_4$. Future theories aimed at describing the high-temperature superconductivity in $YBa_2Cu_3O_{7-y}$ must take into consideration the interlayer interaction mediated by the Cu2-O4-Cu1-O4-Cu2 linkages.

One possible reason for why tetragonal $YBa_2Cu_3O_{7-y}$ ($y > 0.5$) is not superconducting might be that its CuO_2 layer $x^2 - y^2$ band remains half-filled, which requires that the Cu1 atom plane contain the Cu^{3+} and Cu^+ cations in the $(1 - y):y$ ratio. If this is the case, tetragonal $YBa_2Cu_3O_{7-y}$ ($y > 0.5$) would be semiconducting, as shown by van den Berg et al.,[16] and exhibit an antiferromagnetic ordering. We also note that tetragonal $YBa_2Cu_3O_6$ is found to be semiconducting.[6d,7b]

Our calculations of the crystal energies for orthorhombic and tetragonal $YBa_2Cu_3O_{7-y}$ suggest that formation of CuO_3 chains in orthorhombic $YBa_2Cu_3O_{7-y}$ ($y < 0.5$) may arise from two energy factors: to avoid a right-angle arrangement of two oxygen atoms around each Cu1 atom within the Cu1 atom plane and to avoid a T-shape three-coordination for copper. Even for tetragonal $YBa_2Cu_3O_{7-y}$ ($y > 0.5$), these energy factors may still be operative. Thus it is possible that the presence of enough oxygen atom vacancies in tetragonal $YBa_2Cu_3O_{7-y}$ ($y > 0.5$) may allow some short CuO_3 chains to exist and hence some Cu^{3+} sites to form randomly in the two orthogonal directions of the Cu1 atom plane, which leads to a tetragonal structure on a statistical basis.

Acknowledgment. Work at North Carolina State University and Argonne National Laboratory was supported by the Office of Basic Energy Sciences, Division of Materials Sciences, U.S. Department of Energy, under Grant DE-FG05-86-ER45259 and under Contract W-31-109-ENG-38, respectively. We express our appreciation for computing time made available by DOE on the ER-Cray X-MP computer, and would also like to thank Dr. J. D. Jorgensen for preprints of his work, Dr. W. R. Busing for making his WMIN program available to us and also for his invaluable advice concerning how to use it, and Dr. D. Wolf for references.

Contribution from the Department of Chemistry, University of California, Berkeley, California 94720

Ferric Ion Sequestering Agents. 18.[1] Two Dihydroxamic Acid Derivatives of EDTA and DTPA

Petra N. Turowski, Steven J. Rodgers,† Robert C. Scarrow, and Kenneth N. Raymond*

Received November 14, 1986

Two new dihydroxamate analogues of the siderophore aerobactin, derived from the polyamine carboxylate ligands EDTA (ethylenediaminetetraacetic acid) and DTPA (diethylenetriaminepentaacetic acid), have been synthesized. The protonation and stability constants of the ligands and of their complexes with iron(III) have been determined by using potentiometric methods. The number of species in solution and the metal-ligand protonation constants were independently determined by a linear algebraic analysis and least-squares refinement of the visible absorption spectra. The metal-ligand formation constants, K_{ML}, were determined from a similar analysis of the ultraviolet spectra near pH 1. These formation constants [log K values of 30.2 (6) and 29.7 (7), respectively] are higher than usual for dihydroxamate ligands, and there is some evidence that the new ligands may be effective iron removal agents in vivo. The ligands are easily made and purified in large quantities and have desirable solubility properties.

Introduction

We have been involved in the synthesis of ligands that might be useful in the metal chelation therapy of iron overload[2] and, in a related project, the preparation of specific sequestering agents for plutonium.[3] For this purpose, we have looked to the siderophores—a class of molecules produced by microorganisms to acquire sufficient iron for their survival—for examples of highly specific sequestering agents.[4] Two major groups of siderophores are the catecholates, such as enterobactin, and the hydroxamates, exemplified by the ferrioxamines, aerobactin, and others. Our attention has focused mainly on ligands mimicking enterobactin, since it is the strongest iron(III) chelating agent known (log K_{ML} = 52).[5] Unfortunately, such tricatecholate ligands are often difficult and expensive to synthesize and the parent compounds and their ferric complexes are relatively insoluble in neutral and acidic solutions.[6] This is also true for the larger trihydroxamate ligands, since the backbone of such ligands often consists of fairly large nonpolar or only slightly polar chains and rings that enable the chelating moieties to bind all the coordination sites of the metal.

* To whom correspondence should be addressed.
† Deceased.

(1) Part 17: McMurry, T. J.; Hasseini, M. W.; Garrett, T. M.; Hahn, F. E.; Reyes, Z. E.; Raymond, K. N. *J. Am. Chem. Soc.* **1987**, *101*, 7196.
(2) Raymond, K. N.; Chung, T. D. Y.; Pecoraro, V. L.; Carrano, C. J. *The Biochemistry and Physiology of Iron*; Saltman, P., Hegenauer, J., Eds.; Elsevier Biomedical: New York, 1982; pp 649-662.
(3) A discussion of the chemical and biochemical similarities of iron and plutonium may be found in: Raymond, K. N.; Smith, W. L. *Structure and Bonding*; Goodenough, J. B., Hemmerich, P., Ibers, J. A., Jorgenson, C. K., Neilands, J. B., Reinen, D., Williams, R. J. P., Eds.; Springer-Verlag: West Berlin, 1981; Vol. 43, pp 159-186.
(4) A recent review of this may be found in: Raymond, K. N.; Müller, G.; Matzanke, B. F. *Topics in Current Chemistry*; Boschke, F. L., Ed.; Springer-Verlag: West Berlin, 1984; Vol. 123, pp 49-102.
(5) Harris, W. R.; Carrano, C. J.; Cooper, S. R.; Sofen, S. R.; Afdeef, A. E.; McArdle, J. V.; Raymond, K. N. *J. Am. Chem. Soc.* **1979**, *101*, 6097.
(6) Harris, W. R.; Raymond, K. N. *J. Am. Chem. Soc.* **1979**, *101*, 6534.

0020-1669/88/1327-0474$01.50/0